



**HAL**  
open science

## Extraction of mechanical work from stimuli-responsive molecular systems and materials

Alexis Perrot, Emilie Moulin, Nicolas Giuseppone

► **To cite this version:**

Alexis Perrot, Emilie Moulin, Nicolas Giuseppone. Extraction of mechanical work from stimuli-responsive molecular systems and materials. *Trends in Chemistry*, 2021, 3 (11), pp.926-942. 10.1016/j.trechm.2021.08.007 . hal-03418854

**HAL Id: hal-03418854**

**<https://hal.science/hal-03418854v1>**

Submitted on 8 Nov 2021

**HAL** is a multi-disciplinary open access archive for the deposit and dissemination of scientific research documents, whether they are published or not. The documents may come from teaching and research institutions in France or abroad, or from public or private research centers.

L'archive ouverte pluridisciplinaire **HAL**, est destinée au dépôt et à la diffusion de documents scientifiques de niveau recherche, publiés ou non, émanant des établissements d'enseignement et de recherche français ou étrangers, des laboratoires publics ou privés.

# Extraction of mechanical work from stimuli-responsive molecular systems and materials

Alexis Perrot, Emilie Moulin, and Nicolas Giuseppone\*

*SAMS Research Group, Institut Charles Sadron, CNRS, University of Strasbourg,  
67000 Strasbourg, France*

\*Correspondence: giuseppone@unistra.fr

## Keywords

Molecular switches, Molecular motors, Stimuli-responsive materials, Soft actuators

## Abstract

Molecular switches and advanced molecular motors, which are the elementary building blocks for the construction of molecular machines, have been recently integrated into soft materials in order to generate macroscopic actuation under various types of external stimulations. However, to produce a continuous work from these materials, and therefore to potentially achieve more advanced tasks, important structural and dynamic aspects should be considered at all length scales. Here we discuss the implementation of thermodynamic, photodynamic, and dissipative molecular switches and motors in such stimuli-responsive materials. We also highlight the different ratcheting strategies that can be implemented in these actuators to confer them with the capacity of achieving unidirectional cyclic motion, and in order to continuously and autonomously increase their work output.

## 25 **Towards a new generation of molecular systems and materials that can perform mechanical** 26 **tasks**

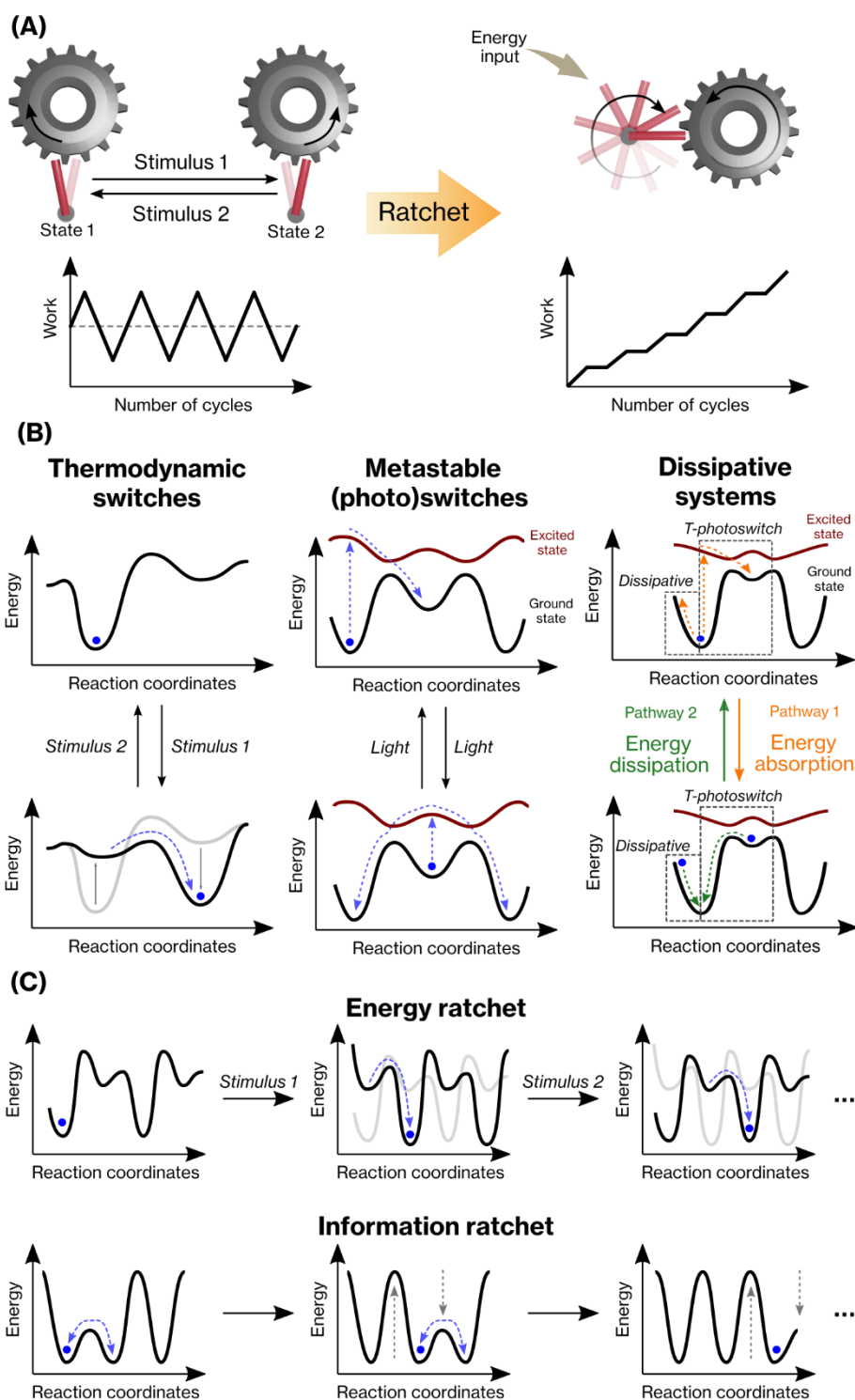
27 Machines convert an input of energy in mechanical forces and movement in order to  
28 perform a task. In our everyday life at macroscopic scale, we are acquainted with machines  
29 consuming electric or thermal energy for transport or automation. At nanoscale, living  
30 organisms also make use of biomolecular machines to function :[1] for instance, kinesin  
31 walkers or salmonella H<sup>+</sup>-driven motor use a chemical fuel (i.e. ATP) for the transportation of  
32 cargos across the cells or for bacterial locomotion.[2,3] In both macro- and nanoscale  
33 machines, the production of a unidirectional and repetitive mechanical actuation (such as a  
34 continuous rotation) is mandatory to constantly increase the work they can produce on their  
35 environment and to achieve complex tasks autonomously. However, if ratcheting devices are  
36 common at macroscale, reaching unidirectional motion in a Brownian environment is a real  
37 challenge which requires a deep thermodynamic control of the molecular actuation.

38 From a chemist point of view, the blossoming development of stimuli-responsive molecules  
39 and materials therefrom is of particular interest to think about the design of new kinds of  
40 mechanically active synthetic systems, capable of controlled actuation at different length  
41 scales by consuming various sources of energy.[4] Nevertheless, the amplification of  
42 nanoactuators up to the macroscopic scale is a difficult objective to reach because it requires  
43 to finely engineer the coupling of dynamic molecular elements in space and time. In addition,  
44 upon energy absorption, the mechanical work done by purely switching molecular actuators  
45 in devices and materials is usually undone when resetting them to their original state due to  
46 **microscopic reversibility** (see Glossary). Therefore, breaking spatial and time-reversal  
47 symmetries in such systems constitute an important challenge for the design of truly **active**  
48 **materials**. [5] In this direction, dissipative out-of-equilibrium “ratcheting” mechanisms must  
49 be implemented during the system’s operation, in order to make use of the mechanical work  
50 generated before the material returns to its starting state.

51 The present Review aims at providing physical and chemical strategies to incorporate  
52 ratcheting mechanisms in the emerging domain of mechanically active molecular materials  
53 (Box 1, Figure I, Key Figure). In a first section, we will survey the diversity of stimuli-responsive  
54 materials that have been designed to generate mechanical motion, since all of them could be  
55 potentially ratcheted. In a second part, we will highlight recent advances in the design of  
56 ratcheting strategies at both the macroscopic and molecular scales in order to extract and

67 exploit mechanical work from actuation cycles. Even though we approach here this topic from  
 68 a synthetic chemist point of view, we also wish to highlight the potential benefit of  
 69 interdisciplinary research to develop the next generation of such active materials.

## Box 1. Thermodynamics of molecular switches and motors



61

62 Upon appropriate stimuli, molecular switches can reversibly evolve between different  
63 states which correspond to local minima of their energy profiles. In general, the switching  
64 process takes place according to two different mechanisms. Either modification of the ground  
65 state energy of the molecule leads to a different stable state, or the switch reaches a  
66 metastable state of higher energy when supplied with energy.

67 In the first case, application of a stimulus changes the energetic profile of the molecule.  
68 Consequently, the initial state is not the most stable one anymore and the system thermally  
69 relaxes to its new thermodynamic equilibrium, whence the term 'thermodynamic switch'  
70 (Figure IB, left). The relative populations of all states are governed by Boltzmann distributions.  
71 Another stimulus can either revert the molecule back to its initial state or lead to another new  
72 thermodynamic equilibrium.

73 The second scenario involves the absorption of energy to reach a metastable state.  
74 Photoswitches follow this mechanism; those molecules absorb photons to reach an excited  
75 state and relax to a metastable state of their ground energy, whence the term 'metastable  
76 switch'. Since this conversion is not governed by thermal processes, the relative populations  
77 of the different states do not follow Boltzmann distributions. From its metastable state, the  
78 switch can reabsorb a photon to go back to its stable ground state through the excited state.  
79 Therefore, by tuning the energetic barrier between the states and working with appropriate  
80 wavelengths, one can reach long half-lives of the metastable configuration and actuate the  
81 molecule between these two states (Figure IB, middle).

82 A third scenario involves so-called dissipative systems which are constantly being driven  
83 out-of-equilibrium by absorbing energy and which are continuously dissipating this energy to  
84 their surrounding when relaxing to their thermodynamically stable state (Figure IB, right). The  
85 out-of-equilibrium state cannot be maintained without energy supply. Photoswitches with  
86 short-lived metastable states are dissipative since the absorption of light energy breaks  
87 microscopic reversibility when the switch concomitantly relaxes back to its global equilibrium  
88 through a low activation barrier of the ground state. Molecular motors are also dissipative  
89 systems, but where the energy dissipation preferentially occurs in one direction by  
90 implementing ratcheting strategies. For instance, dissipative photoswitches change their  
91 geometry during their operation but the molecular motion averages to zero over time; photo-  
92 driven molecular motors, on the other hand, continuously move in one direction and their  
93 motion can therefore be exploited at the nanoscopic scale to produce an increasing work on

94 their environment. Ratcheting strategies can be of different types and involve either *i)* “energy  
95 ratchets” that have no reference to the position of the particle and in which biased potential–  
96 energy minima and maxima are repeatedly modified (Figure 1C, top), or *ii)* “information  
97 ratchets” which rely on modifying the height of an energy barrier depending on the position  
98 of the particle on the potential-energy surface (Figure 1C, bottom).

## 99 **Macroscopic actuation from stimuli-responsive molecular materials**

100 Molecular switches may trigger various changes in chemical and physical properties at the  
101 nanoscale upon appropriate stimulation, and these changes may be in turn amplified – by  
102 diverse processes – up to the generation of macroscopic actuators.[6] As discussed hereafter,  
103 such materials can be synthesized from switches involving thermodynamic, metastable, or  
104 dissipative states (Box 1), and therefore they can differ by the way they use (i.e. absorb and  
105 release) an external source of energy to convert it in molecular motion.

### 106 *Materials based on thermodynamic switches*

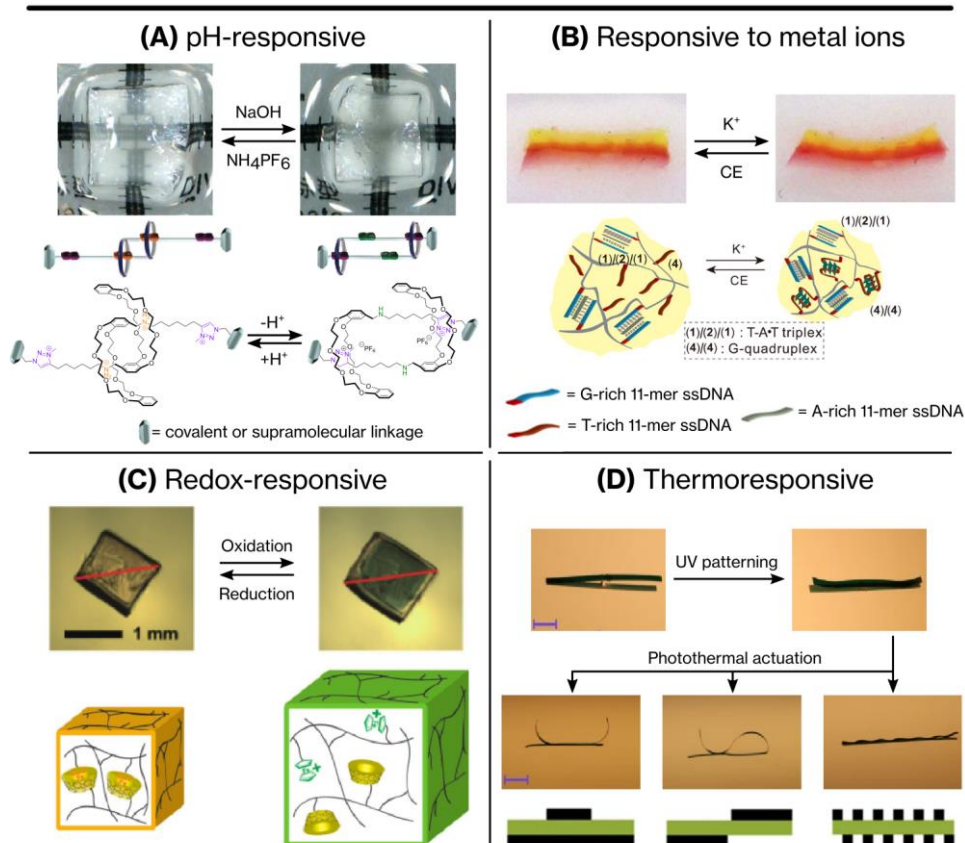
107 The functioning principle of a thermodynamic switch relies on the application of an external  
108 stimulus to alter its ground state energy profile and to shift its thermodynamic equilibrium  
109 (Box 1 and Figure 1B, left). The mechanical motion generated by such switches arises from  
110 their reversible thermal relaxation between an initial state (becoming thermodynamically  
111 unstable) and a final state (becoming thermodynamically stable). While chemoresponsive  
112 switches reach a new stable state upon changes in their chemical environment (such as pH or  
113 metal ions concentration), thermoresponsive switches are based on phase transitions leading  
114 to different temperature-dependent equilibria.

115 Several strategies have been used to design *chemoresponsive (macro)molecular actuators*.  
116 For instance, hydrogels based on pH-responsive polymers have different swelling equilibria  
117 depending on protonation (or deprotonation) of basic (or acidic) side groups. P(HEMA-*co*-AA)  
118 (poly[(2-hydroxyethyl methacrylate)-*co*-(acrylic acid)]) and P(HEMA-*co*-DMAEMA) (poly[(2-  
119 hydroxyethyl methacrylate)-*co*-(2-(dimethylamino)ethyl methacrylate)]) were used to create a  
120 microfluidic valve that could sort aqueous solutions depending on their pH, exploiting the  
121 opposite swelling behavior of these two polymers under basic and acidic conditions [7].  
122 Another strategy consists in using responsive supramolecular units in the system; for instance  
123 by involving DNA sequences which are known to be sensitive to various stimuli [8,9]. In  
124 particular, i-motifs [10,11], which are formed under slightly acidic pH, have been used to

125 design DNA-based bilayered actuators [12]. Upon acidification of the medium, cytosine-rich  
126 DNA sequences form these i-motifs, which act as new physical crosslinks in the hydrogel,  
127 therefore inducing a stress in one layer which bends the entire material. Using more complex  
128 actuating units based on **molecular machines** using **mechanical bonds**, [13,14] our group  
129 developed polymerizable **[c2]daisy chains** to form a contractile gel sensitive to pH changes  
130 (Figure 1A) [15,16]. In basic conditions, the macrocycles preferentially bind the triazolium  
131 stations and the molecule stands in a contracted state; in acidic conditions, however, the  
132 secondary amines are protonated and the macrocycles preferentially bind the  
133 dialkylammonium stations, resulting in an extended conformation. At the molecular scale, this  
134 sliding motion occurs over approximately 1 nm but, when the [c2]daisy chains are polymerized  
135 into a covalent network by copper-catalysed Huisgen[3+2] cycloaddition, the nanometric  
136 displacements are correlated through space and are amplified up to the macroscopic scale.  
137 The [c2]daisy-chain-based gels contract to approximately 60 % of their initial volume in basic  
138 conditions and recover their initial shape in acidic conditions. Metal ions can also trigger  
139 actuation in responsive materials. For instance, guanine-rich DNA sequences are sensitive to  
140 monocationic ions, such as potassium or sodium, leading to the formation of G-quadruplexes.  
141 Following a mechanism similar to the one described for materials based on i-motifs (*vide*  
142 *supra*), bilayered actuators bending upon addition of potassium ions were designed (Figure  
143 1B) [12]. Alternatively, DNA-DNA duplexes with cytosine-cytosine mismatches, which are  
144 sensitive to silver ions, were used to fabricate metal-sensitive hydrogel actuators [17].  
145 Supramolecular redox processes have also been considered as stimuli for actuators. In an early  
146 example, Harada *et al.* developed a hydrogel actuator based on the redox sensitive ferrocene-  
147 cyclodextrin interaction. In reductive conditions, these two molecules form an inclusion  
148 complex in water because of the hydrophobicity of ferrocene. Under oxidative conditions,  
149 however, the ferrocene switches to its cationic ferrocenium ion and electrostatic repulsion  
150 breaks the complex with cyclodextrin. In the hydrogel, oxidation induces a reduction of the  
151 crosslinking density due to the dissociation of inclusion complexes, which results in an  
152 expansion of the material (Figure 1C) [18]. Recently, a similar material based on viologen-  
153 cyclodextrin interactions was reported as redox responsive actuator. In that case, inclusion  
154 complexes consisting of cyclodextrin and dimers made of reduced radical-monocationic  
155 viologen act as additional reticulating units which break upon oxidation, leading to an  
156 expansion of the material [19]. Alternatively, oligoviologen units inserted into a polymeric

157 hydrogel can act by themselves as redox-responsive units. Reduction of the viologens leads to  
 158 the formation of complexes between the reduced radical-cationic species inducing the folding  
 159 of the polymer chains and the subsequent material's contraction [20].

### Thermodynamic switches



160  
 161 **Figure 1. Representative examples of actuators based on thermodynamic switches. (A)** pH-  
 162 responsive chemical gel based on [c2]daisy chains. Under basic conditions, the macrocycles  
 163 preferentially bind the triazolium stations (purple) and the switch is in a contracted conformation. In  
 164 acidic conditions, the secondary amines (green) are protonated and the macrocycles preferentially  
 165 bind the dialkylammonium stations (orange), resulting in an extended state of the [c2]daisy chains.  
 166 The molecular motion is amplified up to the macroscopic scale in the chemical gel. Black ticks in the  
 167 snapshots are separated by 1 mm. **(B)** DNA-based actuator responsive to metal ions and schematic  
 168 representation of the yellow layer. The red layer is mainly composed of PNIPAM, while the yellow layer  
 169 is made of polyacrylamide. Upon addition of potassium ions, the yellow layer can form G-quadruplexes  
 170 which act as new crosslinks, thus leading to a contraction of this layer and, hence, a bending of the  
 171 material. CE stands for crown ether. The length of the gels is ~ 2 cm. **(C)** Redox-responsive actuator  
 172 based on ferrocene-cyclodextrin complexes. In reductive conditions, ferrocene forms inclusion  
 173 complexes with cyclodextrin because of its hydrophobicity; in oxidative conditions, the formation of  
 174 the ferrocenium cation leads to dissociation. As the crosslinking density decreases, expansion of the  
 175 gel occurs. **(D)** Reprogrammable thermoresponsive LCN actuator. An initial reversible photopatterning  
 176 step, leading to a minimal deformation of the material, creates stress distributions in the network.  
 177 Heating the material with light *via* photothermal agents actuates the material following these patterns  
 178 (representation below). Scale bars: 5 mm. *Figure 1A: from 10.1021/jacs.7b06710, Figures 1 and 3.*



179 Figure 1B: from 10.1021/jacs.6b10458, Figure 3. Figure 1C: from 10.1002/anie.201300862, Figure 3.  
180 Figure 1D: from 10.1038/s41467-018-06647-7, Figure 4. The four of them have been adapted.

181

182 Different strategies have also been proposed in order to reach *thermoreponsive actuating*  
183 *devices*. One of them relies on the use of common thermoresponsive polymers such as  
184 PNIPAM (poly(N-isopropylacrylamide)) which displays a **LCST** around 32°C in water, meaning  
185 that its solubility substantially decreases above this temperature. As a result, PNIPAM-based  
186 hydrogels shrink when heated. Recent reports involving PNIPAM include the design of bilayer  
187 composites exhibiting bending motion [12,21,22], and of robotic devices such as grippers that  
188 could reversibly grab and release an object [23]. **Liquid crystalline networks (LCNs)** are also  
189 common thermoresponsive materials where the phase transition between the ordered,  
190 liquid-crystalline phase and the disordered isotropic phase leads to volume changes. Since  
191 light can be precisely addressed spatially and temporally, LCNs are commonly doped with  
192 photothermal agents [24] such as carbon nanotubes [25], gold nanoparticles [26,27] or  
193 organic dyes [28]. While most designs result in bistable actuators, recent reports have shown  
194 reprogrammable systems where different final states can be reached. For instance, Lahikainen  
195 and colleagues reported an azobenzene-based LCN that could be reversibly patterned with UV  
196 light through photomasks. As a consequence, different stress distributions were achieved  
197 inside the material, leading to different deformation modes once the material was heated *via*  
198 **photothermal effect** (Figure 1D) [29]. Recently, incorporation of diarylethene units inside  
199 these LCNs allowed actuation only when both UV and visible light were applied, thereby acting  
200 as an AND logic gate [30]. Finally, Zeng and coworkers reported so-called ‘Pavlovian’ materials  
201 based on LCNs [31] where the material, initially inert to light, could be ‘trained’ to become  
202 light-sensitive by allowing the diffusion of photothermal agents inside the material during  
203 simultaneous heat/light stimulation [32]. Interestingly, DNA-based materials have also been  
204 reported as thermoresponsive actuators. The dissociation of DNA duplexes could be  
205 controlled by heating the material with light using gold nanoparticles or nanorods as  
206 photothermal agents, leading to a change in crosslinking density which triggered actuation  
207 [33]. The reversibility of the DNA complexes formation in the absence of light allowed the  
208 recovery of the initial shape.

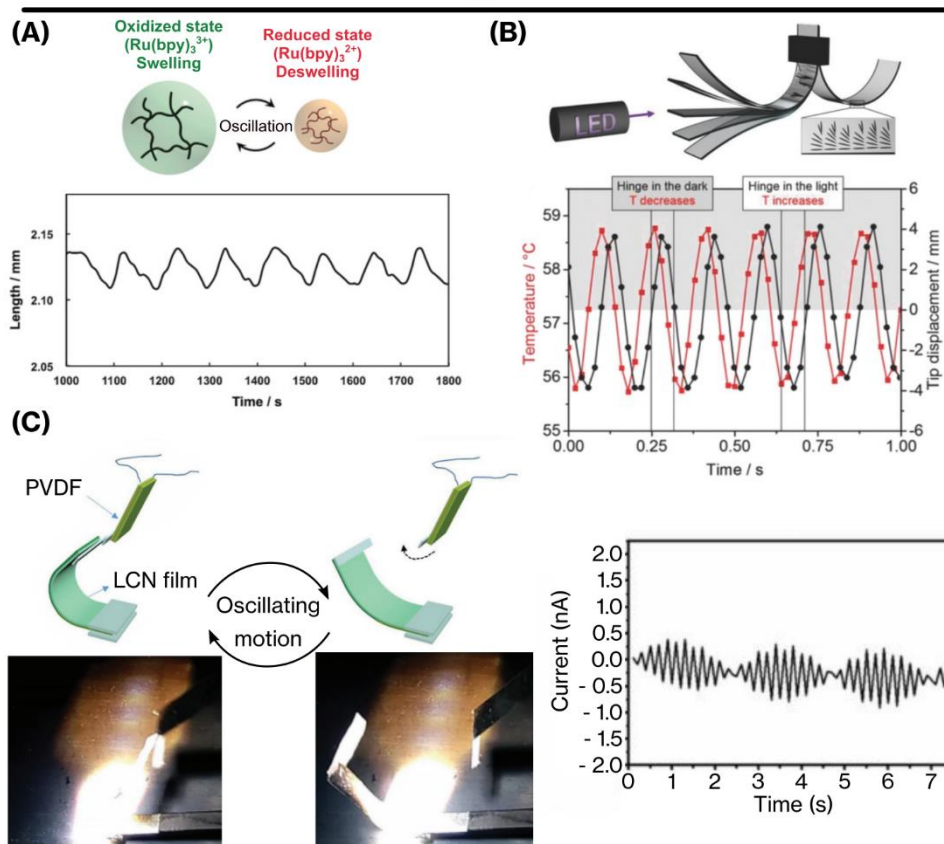
209 *Oscillating phenomena* have also been exploited to trigger back and forth actuation using  
210 either chemoresponsive or thermoresponsive systems. This approach has the advantage of

211 cyclically modulate the global energy profile of a molecular material over time without the  
212 need of sequential inputs. Most oscillating chemoresponsive materials are based on the  
213 **Belousov-Zhabotinsky (BZ) reaction**. For instance, the redox-responsive catalyst of the BZ  
214 reaction can be covalently incorporated inside PNIPAM-based hydrogels. The oscillating  
215 change in hydrophilicity of the catalyst result in an oscillating modulation of the hydration  
216 equilibrium of the polymer, thereby leading to an oscillating volume change of the material  
217 (Figure 2A) [34,35]. An oil pump was recently reported with this type of material [36]. Other  
218 oscillating reactions have also been used to design time-dependent actuating materials [37],  
219 such as an enzymatic oscillating reaction powered by ATP that led to an oscillating  
220 concentration in calcium ions. These ions could reversibly bind to phosphate groups along the  
221 polymer chains of an hydrogel, thereby modulating the crosslinking density and thus inducing  
222 periodic volume changes [38]. Oscillating materials can also be designed from  
223 thermoresponsive materials. The groups of Broer and Meijer thoroughly investigated this  
224 phenomenon with thermotropic LCNs doped with photothermal agents. In this case,  
225 irradiation of the material induces its bending; the bent part, however, blocks the light source  
226 from irradiating the material. It therefore relaxes back thermally to its initial position, allowing  
227 the light source to irradiate again the LCN, which bends again. This self-shadowing effect leads  
228 to a sustained oscillations of the polymer films (Figure 2B) [39–41]. Finally, such a kind of  
229 device can be coupled to another material collecting and transducing the generated  
230 mechanical motion. This was reported, for instance, with oscillating materials driven by  
231 photothermal effect (*vide supra*) and coupled to piezoelectric PVDF (poly(vinylidene fluoride))  
232 films [42]. The observed piezoelectric effect arises from the oscillation of the PVDF film, which  
233 comes from the light-induced oscillatory motion of an LCN material. Consequently, the  
234 oscillating motion of the LCN is transduced, *via* the PVDF, as an oscillating potential difference  
235 between two electrodes. It is worth noting that this potential difference averages to zero over  
236 time, highlighting that, overall, no continuous work is extracted (Figure 2C).

237 Although thermodynamic switches allow the design of a wide variety of materials, they are  
238 often associated with several drawbacks. Chemoresponsive systems usually suffer from  
239 substantial fatigue after a few operating cycles because of the accumulation of chemical waste  
240 over time. Thermoresponsive materials, on the other hand, cannot be directly addressed very  
241 precisely with temperature, thus requiring very often the use of photothermal agents, since

242 light can be more easily focused on precise spots at precise times. In the following section, we  
 243 will see how light can be used to actuate materials following totally different energy profiles.

### Oscillating materials



244  
 245 **Figure 2. Representative examples of oscillating materials.** (A) Microgels based on PNIPAM were  
 246 functionalized with tris(bipyridine)ruthenium ( $\text{Ru}(\text{bpy})_3$ ). Since it is swollen in a BZ reaction medium,  
 247 the oxidation state of  $\text{Ru}(\text{bpy})_3$  cyclically changes over time and, hence, modifies the hydration  
 248 equilibrium of the polymer gel (top). Consequently, the microgels cyclically swell and shrink over time  
 249 (bottom). (B) LCNs with a splay alignment were doped with photothermal agents (top). Upon local  
 250 irradiation, the photothermal effect from the dopants induces local heating of the material and,  
 251 therefore, its bending. Consequently, the tip of the LCN films blocks the light beam from reaching its  
 252 irradiation point; rapid heat dissipation triggers the unbending of the material to its initial state and  
 253 the cycle is repeated (bottom). (C) Oscillating LCN films were used to modulate the potential difference  
 254 between two electrodes. The oscillating motion of the light-sensitive was used to hit a PVDF film and  
 255 induce its own mechanical oscillation (left). The oscillating deformation of the PVDF creates an  
 256 oscillating potential difference between two electrodes (right). The ‘beating’ aspect is caused by a  
 257 mismatch between the oscillation frequency of the LCN and the oscillation frequency of the PVDF (due  
 258 to its intrinsic elasticity). Importantly, the potential difference averages to zero over time. *Figure 2A;*  
 259 *from 10.1002/anie.201809413 Figures 1 & 5. 2B: from 10.1002/adma.201606712, Figure 2. 2C: from*  
 260 *10.1002/adom.201800131, Figure 6.*

261

## 262 *Materials based on metastable switches*

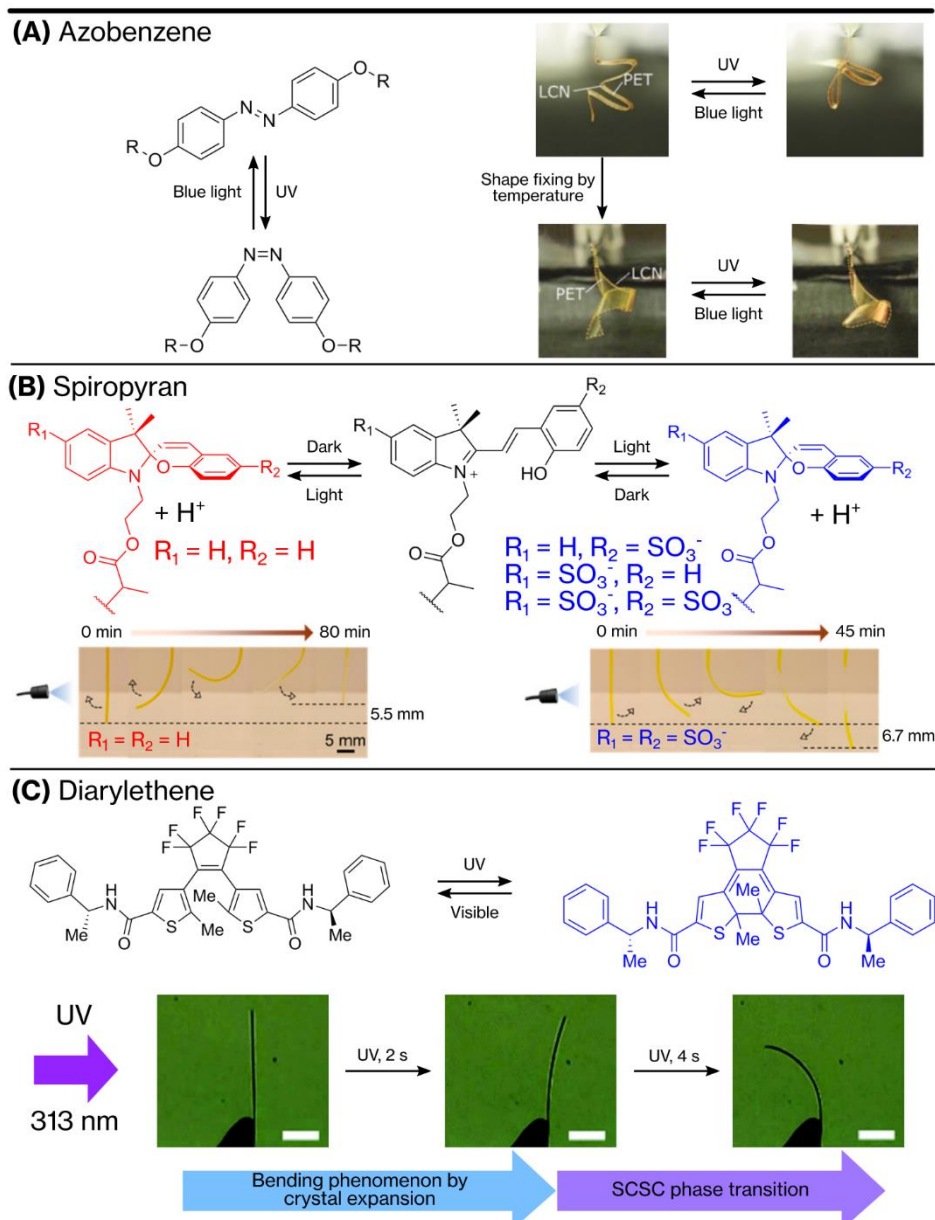
263 Under light irradiation, photoswitches can reach a metastable state of higher energy (Box  
264 1 and Figure IB middle), thus leading to a state probability inaccessible for thermodynamic  
265 switches following Boltzmann distribution. This excitation process is photodynamic as it is  
266 reversible through the excited state between the metastable and stable ground states. In  
267 addition, this reversibility can be complemented by a thermal process going from the  
268 metastable state to the stable one when the energy barrier of the ground state is low enough  
269 to be crossed, thus leading to dissipative systems which can be maintained out-of-equilibrium  
270 under light irradiation (Box 1 and Figure IB, right). Note that such photoswitching systems do  
271 not follow the principle of microscopic reversibility, and as it is the case for switches purely  
272 actuating back and forth along their ground states such as chemical systems displaying  
273 **detailed balance**. Consequently, an actuating material based on photoswitches can reach,  
274 depending of the height of the ground state energy barrier, either a metastable shape that  
275 can be reset by photoexcitation, or an out-of-equilibrium shape that eventually relaxes back  
276 thermally.[43] Several molecular photoswitches have been recently implemented to access  
277 actuating macroscopic materials [44,45].

278 *Azobenzene derivatives* are probably the most used ones. Upon light irradiation, the stable  
279 *trans*-isomer is isomerized to its metastable *cis*-form. This process is reversible either by  
280 thermal relaxation or by light irradiation [46]. *Trans*-azobenzene, with an elongated shape,  
281 has been widely used as dopant in LCNs which can then actuate according to either a  
282 photothermal or a photomechanical mechanism. On one hand, since azobenzene absorbs  
283 light, it can be used as a photothermal agent to trigger the actuation of thermoresponsive  
284 LCNs by the photothermal effect. On the other hand, the photomechanical effect, which arises  
285 from the bent structure of the *cis*- isomer, can induce destabilization of the liquid crystalline  
286 phase leading to disorder which results in a volume change of the material. However, the  
287 relative contribution of each mechanism is still a subject of investigations [47]. LCNs have great  
288 potential to be used in soft robotics because of their mechanical properties and their efficient  
289 stimuli-responsiveness; therefore, doping them with light-sensitive molecules paves the way  
290 towards remotely controlled soft robotics systems.[48,49] While most azobenzene-based  
291 LCNs lead to materials which can actuate between two states [50], recent reports presented  
292 reprogrammable materials including for instance liquid crystalline elastomers [51] or  
293 LCN/thermoplastic composite materials [52]. In this last example, the presence of a

294 thermoplastic polymer allows for shape molding and reprogramming at a temperature close  
295 to the glass transition temperature while light is used for actuating the LCN (Figure 3A) [52].  
296 Recent developments also include the design of more complex materials that are multi-stimuli  
297 responsive [53,54] or that can get crossed-information from the environment to trigger their  
298 actuation [55]. Azobenzenes in their *trans*- form are also known to form inclusion complexes  
299 with cyclodextrins [56]. Upon UV light irradiation, the formation of the *cis*- isomer leads to the  
300 dissociation of the complex. This unthreading process that has been exploited in chemical gels  
301 based on [c2]daisy chains [57] and **[2]rotaxanes** [58] leads to a volume change of the material  
302 upon light irradiation.

303 *Spiropyran* has also been widely used for the design of photoactuated materials [6,59].  
304 Under light irradiation, it can reversibly isomerize between its closed spiropyran form and its  
305 open merocyanine form. The stimuli-responsiveness of spiropyran-based materials originates  
306 from the difference in polarity between these two isomers. In water, in the absence of any  
307 charged substituents, the zwitterionic merocyanine is the most stable isomer and its ring  
308 closure under light irradiation leads to the neutral spiropyran, which is less solvated by water.  
309 When incorporated in a hydrogel, this change in solubility induces a shrinkage of the material  
310 upon light irradiation, subsequently leading to a bending towards the light source [60]. This  
311 tendency can be reversed if the spiropyran is functionalized with negatively charged sulfonate  
312 groups which increase the net charge of the molecule in its closed form (Figure 3B) [61]. As  
313 for azobenzene, new materials with improved performance are still regularly reported. For  
314 instance, the group of Stupp designed a hybrid hydrogel made of supramolecular nanofibers  
315 that are chemically cross-linked to a photo-responsive chemical network containing  
316 spiropyran side chains [62]. As a gradient of hydrophobicity occurs upon light irradiation, a six-  
317 arm flower-shaped hydrogel was bent in different configurations by precisely addressing the  
318 light on each petal.

## Metastable switches



319

320 **Figure 3. Representative examples of actuators based on metastable switches. (A)** Reprogrammable  
 321 azobenzene-based LCN. The LCN is prepared on a thermoplastic substrate (PET, poly(ethylene  
 322 terephthalate)) that can be deformed when heated above its glass transition temperature. Different  
 323 modes of actuation under UV light can therefore be achieved with a single material. The length of the  
 324 material is 2 cm. **(B)** Spiropyran-based gels. When merocyanine has no sulfonate group, ring closure  
 325 under UV decreases the net charge of the molecule, leading to a contraction towards the light source.  
 326 Yet, when merocyanine has sulfonate groups, ring closure under UV increases the net charge of the  
 327 molecule, leading to an expansion of the gel and, therefore, a bending motion away from the light  
 328 source. In both cases, for prolonged irradiation times, unbending occur as the deformational gradient  
 329 disappears. **(C)** Diarylethene-based crystal. The crystal is irradiated from the left side. Under UV, the  
 330 crystal first bends away from the light source because of the change in geometry of the photoswitch  
 331 which leads to an expansion of the crystal. For longer irradiation times, however, the higher population  
 332 of photocyclized molecules triggers a single-crystal-to-single-crystal transition with smaller final lattice

333 parameters, leading to a bending motion towards the light source. Scale bars: 250  $\mu\text{m}$ . Figure 3A: from  
334 10.1002/anie.201915147, Figure 4. Figure 3B: from 10.1021/jacs.0c02201, Figure 4. Figure 3C: from  
335 10.1039/D0SC05388K, Figure 1.

336

337 *Diarylethenes* can also be used to generate mechanical work because light irradiation  
338 triggers the electrocyclization of the molecule. When organized in crystalline lattices, this  
339 change in geometry can be translated up to the macroscopic scale by reorganization of the  
340 irradiated crystalline phase. Since the first report in 2007 [63], many more systems have been  
341 described (Figure 3C) [64–66].

342 In the first part of this Review, we have discussed different mechanisms that can be used  
343 to generate mechanical actuation from molecular materials. However, in most cases, the work  
344 performed during the actuation comes undone when the material returns to its initial state.  
345 In order to extract increasing amount of work from such materials and to use repeatedly the  
346 mechanical work produced to perform a task, one should enforce them to undergo  
347 unidirectional motions by “ratcheting” their actuations.

### 348 **Extracting continuous mechanical work from molecular systems and materials by** 349 **implementing ratchet mechanisms**

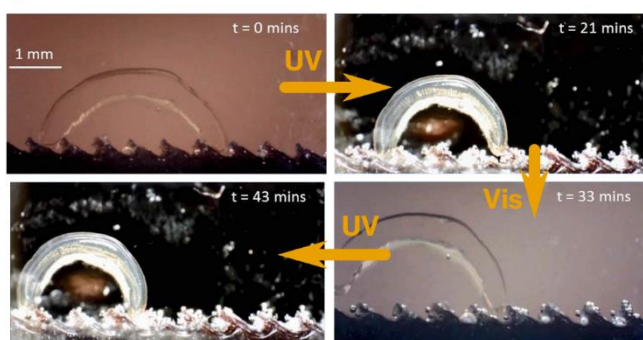
350 To produce a continuously increasing mechanical work on its environment, an actuator must  
351 involve a symmetry-breaking process, as the system must follow a distinct trajectory when  
352 returning back to its initial stable state (Box 1 and Figure 1A, right). Symmetry breaking of  
353 actuating molecular materials can take place by implementing different types of **ratchets**  
354 acting at different length scales. They can for instance (i) take advantage of an asymmetric  
355 external stimulation; (ii) involve a built-in asymmetric response of the material, or (iii) rest on  
356 the design of a ratchet mechanism at the nanoscale in order to upgrade molecular switches in  
357 **molecular motors** (Box 1 and Figure 1C).[67,68]

358 *Asymmetric interaction with the environment.* One possibility to achieve unidirectional motion  
359 of an actuating material is to make it interacting with a ratcheted surface, as already  
360 demonstrated with spiropyran-based gels [69,70]. Oriented translational motion as well as  
361 rotation over several cycles was reported for such materials [62]. A bent gel was also cyclically  
362 swollen and shrunk with light on an asymmetric ratcheted surface (Figure 4A). The  
363 dissymmetric geometry of this serrated surface precluded motion to the right, thus forcing  
364 the material to repeatedly move in the same left direction under sequential light irradiation

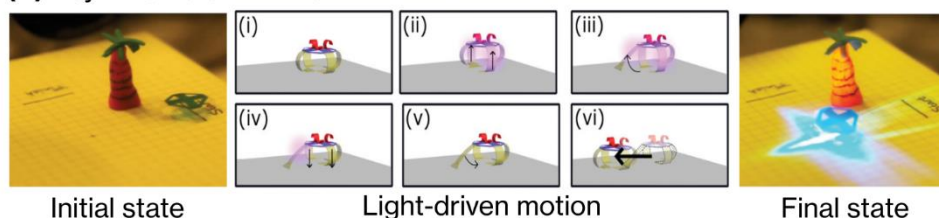
365 [69]. An alternative strategy consists in an asymmetric stimulation of the actuating system.  
 366 Early reports show that either simultaneous or alternate UV and visible light irradiation could  
 367 induce the rolling motion of a belt made of azobenzene-based LCNs [71] or of a gear using  
 368 diarylethene-based crystals, respectively [72]. Recently, Pilz da Cunha *et al.* reported a soft  
 369 robotic tetrapod with four LCN legs that could move and transport objects by selective and  
 370 sequential irradiation of the legs (Figure 4B) [73]. Fischer and coworkers reported the  
 371 translational motion of a tubular LCN caused by a wave-like propagation of a local expansion  
 372 of the material. Light irradiation was locally applied progressively along the length of the  
 373 network, biomimicking the motion of earthworms (Figure 4C).[74]

### Macroscopic ratchets

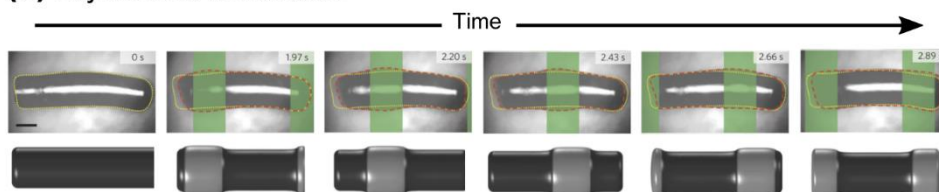
#### (A) Ratcheted surfaces



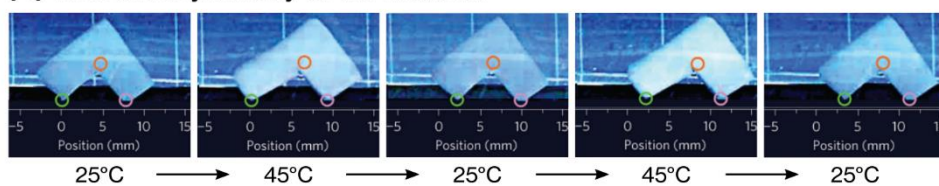
#### (B) Asymmetric stimulation



#### (C) Asymmetric stimulation



#### (D) Inherent asymmetry of the material



374

375 **Figure 4. Design of macroscopic ratchets. (A)** Spiropyran-based gel ‘walking’ on a ratcheted surface.  
 376 The material itself is cycling between two shapes, while the asymmetry of the surface makes it move



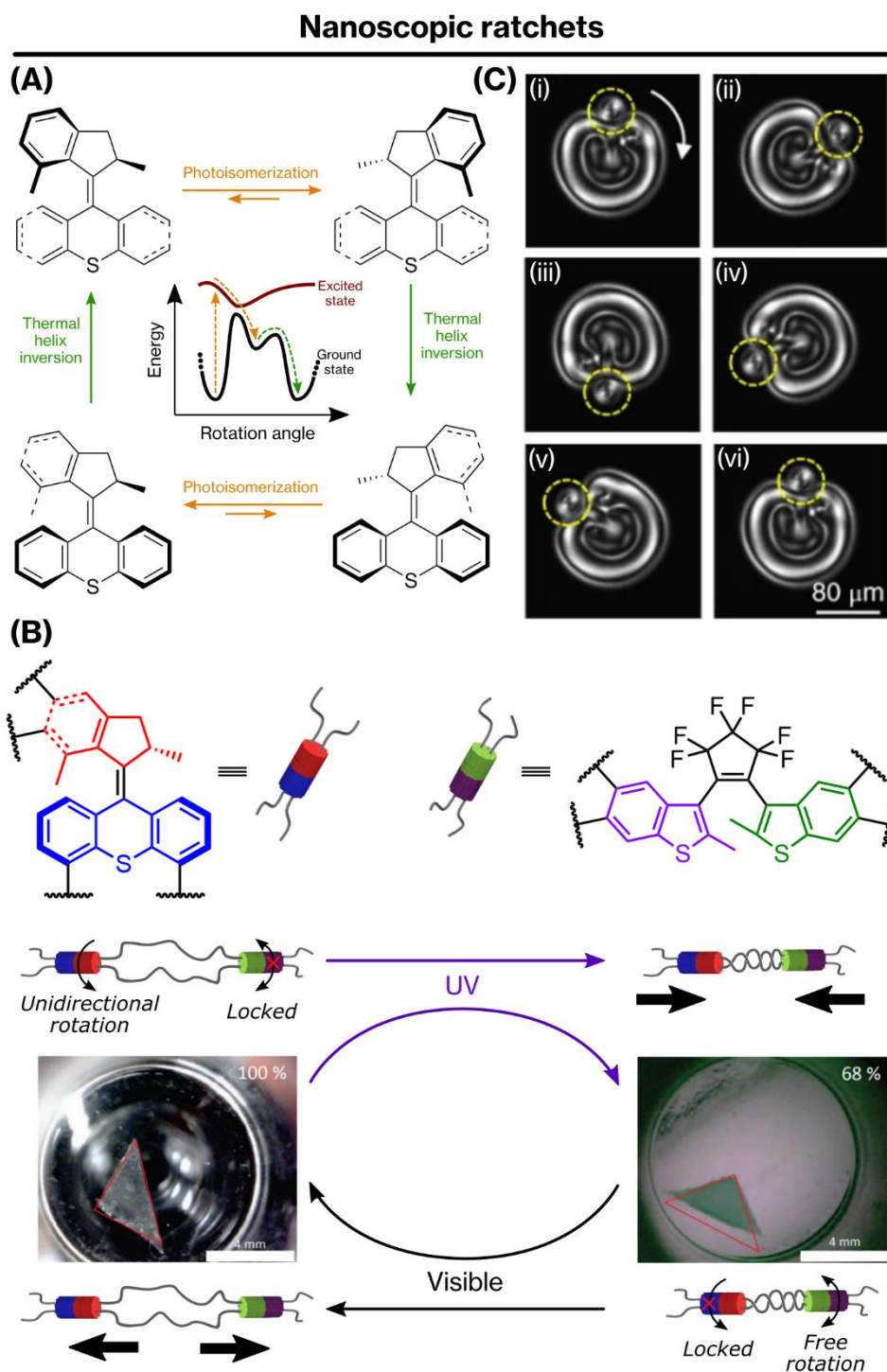
377 preferentially to the left. **(B)** Locomotion of a soft robotic device over more than 4 mm by asymmetric  
378 light stimulation according to the following mechanism: (i) a platform is mounted on four azobenzene-  
379 based LCN 'legs', (ii) irradiation of two opposite legs lifts the device while (iii) irradiation of a third leg  
380 with a tilted angle induces unfolding, (iv) stopping irradiation on the two opposite legs lowers the  
381 platform, (v) light removal from the third leg induces bending back to its initial shape, and (vi) a  
382 translating motion occurs as this bending motion drag the whole system. Snapshots on the left and  
383 right sides show the position of the platform before and after this sequence, respectively. **(C)**  
384 Snapshots of an LCN-based tubular material (top) with the corresponding schematic representation of  
385 the volume changes (bottom). Asymmetric light irradiation leads to the directional motion of the  
386 material. Local light irradiation (green areas) trigger volume expansion. The light beam travels along  
387 the length of the material, causing a wave-like propagation of the deformation, which in turn induces  
388 the translational motion of the tube, similar to the one of an earthworm. Scale bar: 200  $\mu\text{m}$ . **(D)**  
389 Anisotropic PNIPAM-based gel containing precisely-oriented titanate nanosheets. The anisotropic  
390 swelling behavior drives the motion of the gel preferentially to the right side when the temperature is  
391 cycled above and below the LCST. Figure 4A: from 10.1016/j.snb.2017.05.005, Figure 5. Figure 4B: from  
392 10.1002/adv.201902842, Figure 3. Figure 4C: 10.1038/nmat4569, Figure 2 Figure 4D: from  
393 10.1038/nmat4363, Figure 5.

394  
395 *Inherent asymmetry of the macroscopic material.* An alternative approach to extract  
396 mechanical work consists in using materials that are inherently asymmetric at macroscopic  
397 level. For instance, Kim and coworkers developed a PNIPAM-based gel containing  
398 macroscopically aligned titanate(IV) nanosheets, and which displays an anisotropic  
399 thermoresponsive swelling behavior. Interestingly, directional motion of a L-shape cut  
400 material occurred upon heating/cooling cycles, resulting from the anisotropic shape change  
401 which leads to an unidirectional translation of the centroid of the gel (Figure 4D) [75].  
402 Microplatelets coated with azobenzene have been reported to perform continuous rotation  
403 under light irradiation when immersed in a liquid crystal. A feedback mechanism takes place  
404 between azobenzenes and mesogens at the interface of the object, modulating the effective  
405 light beam irradiating the material and, therefore, leading to an unidirectional rotation of the  
406 platelets [76]. Recently, photoresponsive micrometer-sized crystals capable of continuous,  
407 unidirectional twisting motion were reported. Light-induced  $E \rightarrow Z$  isomerization of the  
408 allylidene malonitrile induced disruption of the crystalline phase of the material which  
409 resulted in anisotropic stresses leading to motion [77].

410 *Ratcheting at the nanoscale: molecular motors.* As already discussed, switches can reach  
411 several global or local minima of their energy profile depending on the stimulus applied (Box  
412 1). A peculiar situation arises when the high energy state of a switch (pathway I) is  
413 continuously populated by energy absorption, and continuously depopulated by thermal

414 energy transfer to its surrounding (pathway II) (Box 1 and Figure IB, right). Here, the resulting  
415 out-of-equilibrium situation can be ratcheted if the energy dissipation is enforced to occur in  
416 one preferential direction by molecular symmetry breaking, leading to a so-called molecular  
417 motor capable of unidirectional nanoactuation (Box 1, Figure 1C). Therefore, in contrast to  
418 mechanical switches which influence their surrounding environment as a function of their  
419 states, molecular motors move their subcomponents along a nonreversible energy profile,  
420 and influence their surrounding environment as a function of their trajectory. This confers  
421 them with the unique property to progressively and repeatedly increase the work they can  
422 perform on their environment. For instance, the group of Leigh reported the first chemically  
423 fueled molecular motor prepared from a **[2]catenane** [78]. Proper design of this interlocked  
424 structure allowed the unidirectional chemically powered rotation of one macrocycle with  
425 respect to the other by involving an information ratchet mechanism.[79] Nevertheless, most  
426 synthetic molecular motors are concomitantly photo- and thermally actuated with a  
427 ratcheting mechanism involving the presence of stereogenic centers.[80] The most common  
428 molecules of this type are overcrowded alkenes initially developed by the group of Feringa  
429 (Figure 5A) [81]. In such molecular motors, a first photochemical *trans*→*cis* isomerization  
430 takes place, leading to an unstable helical conformation which can relax to a stable one by  
431 thermal atropisomerization, thus leading to a net 180° rotation. This thermal helix inversion  
432 step is biased towards one particular direction due to the presence of an asymmetric carbon  
433 recovering its favored pseudo-axial conformation from an unfavored pseudo-axial one as  
434 obtained after light-irradiation. The repetition of these two steps completes a net  
435 unidirectional 360° rotation. More recently, hemithioindigo motors have been developed,  
436 following the same mechanistic principles but rather being driven by visible light [81]. In these  
437 motors, the ratchet mechanism is encoded in the molecule itself. If such molecular motors are  
438 still not often exploited to extract mechanical work at higher length scales in materials, a  
439 number of innovative examples exploit the change in geometry at the photostationary state  
440 reached after irradiation. For instance, when overcrowded alkenes are used as chiral dopant  
441 in a liquid crystal, irradiation produces a change in the helicity of the motors, leading to the  
442 deformation of the cholesteric LC phase and subsequently inducing the rotation of a nanorod  
443 on the surface. Then, stopping the irradiation reverts the motion, cancelling the initial work  
444 produced through a reverse rotation of the nanorod [82]. The group of Feringa also reported  
445 supramolecular fibers containing amphiphilic overcrowded alkenes, where irradiation led to

446 bending towards the light source due to a structural disordering of the supramolecular packing  
447 [83–85].



448  
449 **Figure 5. Design and application of molecular motors.** (A) Mechanism for the unidirectional rotation  
450 of second-generation light-driven rotary motors based on overcrowded alkenes. It consists of two  
451 photochemical steps and two thermal isomerization steps. In the most stable configuration, the methyl  
452 group of the asymmetric carbon of the upper part has a pseudoaxial conformation. After the  
453 photoisomerization steps, the motor has an opposite helicity and, in this configuration, this methyl  
454 group has a less stable pseudoequatorial position. The most stable conformation is restored after

455 thermal helix inversion. This ratcheted design of the molecule leads to unidirectional rotary motion.  
456 **(B)** Snapshots and schematic representation of chemical gels formed by rotary molecular motor  
457 crosslinks (red and blue cylinders) and diarylethene-based elastic releasers (purple and green  
458 cylinders). Upon UV irradiation, motors twist pairs polymer chains together, increasing the number of  
459 physical crosslinks and, hence, reducing the volume of the gel. The elastic energy stored in the material  
460 from the torque produced by the molecular motors can be restored upon visible light irradiation over  
461 48 hours, as diarylethene units switch to their open form that can freely rotate and untwist the chains,  
462 recovering the initial volume of the gel. In other words, under UV, the work performed by the  
463 unidirectional motion of motors can be stored in the material because the diarylethenes are in their  
464 closed, 'locked' conformation. However, under visible light, the diarylethene modulators isomerize to  
465 their open form with free rotation around single bonds. Consequently, they will tend to rotate in the  
466 opposite direction to that of the motors to untwist the polymer chains. Overall, the process describes  
467 a continuous and unidirectional trajectory to be activated and reset. **(C)** Liquid-crystalline pattern  
468 continuously rotating under irradiation inside a molecular-motor-doped liquid crystal. The pattern is  
469 observed by polarized optical microscopy between crossed polarizers. The rotation of the pattern rises  
470 from a diffusion-driven feedback process occurring when the motor is isomerized. The torque  
471 produced can be used to transport a microscopic object (circled by yellow dotted line). Full rotation  
472 takes place in ~23 minutes (from (i) to (vi)). *Figure 5B: from 10.1038/nnano.2017.28, Figure 1 and*  
473 *Supplementary Figure 4. Figure 5C: from 10.1038/s41565-017-0059-x, Figure 5.*

474  
475 Our group reported on the formation of chemical gels incorporating such molecular motors  
476 as active crosslinks, and in which the work produced by each motor is directly stored as elastic  
477 energy in the network [86]. Indeed, because the rotation of the motors under UV irradiation  
478 induces a twisting of pairs of polymer chains, the increasing number of crosslinks from  
479 entanglements triggers a contraction of the material (through syneresis), together with an  
480 increase of its elastic modulus [87]. Interestingly, this elastic energy can be released by  
481 integrating light-triggered diarylethene moieties as additional crosslinking units, and through  
482 unwinding of the polymers chains. Because this unwinding take place at a different  
483 wavelength and in different locations of the materials, the entire system can be maintained  
484 out of thermodynamic equilibrium and ratcheted by the opposite directional rotation of the  
485 molecular motors (for instance turning clockwise) and molecular releasers (enforced to  
486 conversely turn anticlockwise) (Figure 5B) [88]. Therefore, the materials as a whole can  
487 contract and expand as a function of the trajectories and the frequencies of its molecular  
488 components and can be considered as intrinsically motorized. Using a different approach,  
489 Katsonis and Brasselet exploited the change in helicity of the molecule during the rotation of  
490 the motor, coupled to a diffusion-driven feedback mechanism, to create a continuously  
491 rotating pattern inside a liquid crystal under light irradiation. The torque produced was used

492 to transport a cargo at microscale (Figure 5C) [89]. Irradiation of the motor leads to  
493 concentration gradients of its different states inside the liquid crystalline medium. In return,  
494 these concentrations gradients form different supramolecular structures between the motors  
495 and the liquid crystal that create a diffusion gradient inside the material. The interplay  
496 between concentration gradients and diffusion gradients leads to the formation of patterns  
497 that break their axial symmetry above a critical power, which then lead to the rotation of the  
498 pattern over time. While the unidirectional rotation of the motor is not directly responsible  
499 for the rotation of the liquid crystalline medium, it still highlights the potential application of  
500 the changes in helicity of the motor during its rotation cycle to design complex stimuli-  
501 sensitive supramolecular systems. These two last examples pave the way to the integration of  
502 molecular motors in globally dissipative systems in order to ratchet molecular materials at all  
503 scale.

#### 504 **Concluding remarks and future perspectives**

505 The recent advances in the design and synthesis of mechanically active molecular materials  
506 are of both fundamental and practical interests. In particular, numerous progresses have been  
507 made by incorporating stimuli-responsive molecular units into polymer matrices. The various  
508 natures of these molecules permit to actuate materials using different sources of chemical or  
509 physical energy. As detailed above, the generated actuation can take place by several  
510 fundamentally distinct mechanisms leading to important thermodynamic consequences at all  
511 scales. One of the challenges in this approach is now to generate materials that can produce  
512 a continuous work on their environment, which requires the implementation of ratcheting  
513 strategies. With the recent development of ratcheting mechanisms at the nanoscale and the  
514 rise of molecular motors, new opportunities appear to exploit the work they can continuously  
515 produce at nanoscale by its amplification in macroscopic materials. A few examples have  
516 already shown that the ratcheted actuation of molecular motors can be preserved in properly  
517 designed artificial materials, but basically everything remains to be explored in this new kind  
518 of integrated motorized molecular systems. In particular, the rationalization of the ratcheting  
519 amplification from nano- to macroscale should be understood and generalized. Their full  
520 potential in terms of non-classical actuation and efficiency should also be clarified in  
521 comparison with simpler switching systems. In this direction, a number of stimulating

522 challenges are certainly facing synthetic chemists and their colleagues at the interfaces with  
523 physics and engineering for the years to come (see Outstanding Questions).

524

## 525 Glossary

526 **[2]catenane:** mechanically interlocked structure composed of two intertwined  
527 macrocycles. The term is derived from the Latin for “chain” (catena).

528 **[2]rotaxane:** mechanically interlocked structure composed of dumbbell shaped molecule  
529 threaded through a macrocycle. The term is derived from the Latin for “wheel” (rota) and  
530 “axle” (axis).

531 **Active material:** material that can perform a task by energy dissipation from its  
532 environment. In particular, when such materials can sense and adapt to what happens in their  
533 environment, when they display motility, or if they reorganize themselves to perform multiple  
534 tasks, they are sometimes named as “life-like” materials.

535 **BZ reaction:** Belousov-Zhabotinsky reaction; an oscillating redox reaction taking place in  
536 acidic aqueous solution in the presence of bromine derivatives, transition metal catalysts and  
537 reducing agents, and driven by non-linear thermodynamics.

538 **[c2]daisy chain:** mechanically interlocked rotaxane composed of two identical molecules  
539 consisting of a ring (macrocycle) covalently linked to an axle. The axle of one molecule is  
540 threaded through the macrocycle of the other one, thereby leading to a cyclic topology [c2].

541 **Detailed balance:** principle stating that, at equilibrium, every process occurs at the same  
542 rate than its reverse process. This principle is therefore tightly related to microscopic  
543 reversibility.

544 **LCN:** Liquid Crystalline Network; a polymer network composed of mesogenic units. The  
545 phase transition from the ordered mesophase to the disordered isotropic phase leads to  
546 volume expansion when the material is heated. Cooling the material back to its liquid  
547 crystalline phase allows the recovery of its initial shape.

548 **LCST:** Lower Critical Solution Temperature; critical temperature under which a polymer is  
549 fully miscible in a solvent, for any composition. Conversely, the UCST (Upper Critical Solution  
550 Temperature) is the critical temperature above which a polymer is fully miscible in a solvent,  
551 for any composition. Crossing these critical temperatures can lead to macroscopic  
552 shrinkage/expansion of the polymer materials.

553 **Mechanical bond:** entanglement in space between two or several molecular components  
554 and that cannot be undone without breaking a covalent bond. Among the possible  
555 mechanically interlocked structures, there are catenanes and rotaxanes, for instance.

556 **Microscopic reversibility:** principle stating that, the probability of any trajectory of a  
557 microscopic process through phase space equals that of the time reversed trajectory. It is  
558 tightly related to detailed balance for chemical reactions at equilibrium.

559 **Molecular machine:** molecular assembly that can perform a task through the controlled  
560 mechanical actuation of its elementary parts under an appropriate stimulus.

561 **Molecular motor:** molecule capable of repetitive directional motion when fueled with a  
562 source of energy. There can be linear molecular motors, like molecular walkers, or rotary  
563 molecular motors, like motors based on overcrowded alkenes. The unidirectionality is  
564 provided by a 'ratcheting' mechanism contained within the molecular motor.

565 **Photothermal effect:** phenomenon where a material emits heat after being excited by light  
566 irradiation.

567 **Ratchet:** macroscopically, a ratchet is a device with asymmetric teeth that bias its continuous  
568 motion in one preferential direction (because preventing motion in the opposite direction).  
569 By analogy, at the nanoscopic scale in Brownian environment, ratcheted energy profiles are  
570 asymmetric and can therefore drive the net unidirectional motion of a system when pumping  
571 energy from their environment. In particular, mechanically active molecular systems can make  
572 use of such ratcheting strategies to continuously move a particle up to an energy gradient.

573

## 574 Highlights

575 A wide variety of stimuli-responsive materials has been recently developed. In particular,  
576 the integration of thermodynamic or photodynamic molecular switches in appropriate  
577 materials can trigger their macroscopic actuation, possibly in combination with oscillating  
578 phenomena.

579

580 Most of these systems, however, cannot progressively perform work on their environment  
581 because they lack spatial asymmetry in their actuation trajectory. Consequently, any work  
582 done in one direction is cancelled once the systems return to their initial state. To create

583 actuators that can produce continuous work, ratcheting strategies must be implemented to  
584 break the spatial symmetry during their operation.

585

586 Macroscopic ratchets can be designed by coupling the whole material with an engineered  
587 asymmetric environment during its actuation. Moreover, ratcheting mechanisms can also be  
588 implemented in dissipative systems at nanoscale by breaking the spatial symmetry of  
589 molecular switches' energy profile, thereby accessing molecular motors.

590

## 591 Outstanding Questions

592 Will the integration of molecular motors in macroscopic materials be limited to a few and  
593 very specific examples, or can it be implemented by the design of more general and  
594 rationalized approaches? In particular, how to preserve – or even amplify –, up to the  
595 macroscopic scale, the dissipative out-of-equilibrium ratcheting actuation of a molecular  
596 motor when integrated in a material?

597 Which efficiency can be reached by these systems, in terms of energy conversion, motion's  
598 trajectory, workload, speed of actuation, and power? Would these materials present clear  
599 advantages compared to simpler switching materials in terms of functioning autonomy and  
600 work production?

601 Are chemically fueled molecular motors capable of integration in actuators? Although  
602 famous examples in biology teach us that this is physically possible, how can we simplify  
603 enough artificial systems to make them accessible to synthetic chemists while keeping enough  
604 functional efficiency?

605 How to couple such molecularly motorized materials with appropriate devices in order to  
606 transduce their mechanical actuation in other types of energy? How to integrate them with  
607 other molecular elements (or macroscopic segments) to access multitasking materials? How  
608 to engineer them and to interface them with their environment in order to control them  
609 and/or to generate autonomous feedback loops leading to adaptation? Can we push such  
610 systems sufficiently far away from equilibrium to generate self-organizing emergent behaviors  
611 (reaching for instance bifurcation points in their trajectories)?



612 Can we make such materials cheap and sustainable enough for useful applications, in  
613 particular by simplifying their chemical structures and by improving their resistance to  
614 fatigue?

615 What could be the potential applications of such materials going from energy storage and  
616 catalysis, to soft robotics and medicine? Can they become essential part of more complex  
617 intelligent materials?

618

## 619 **Acknowledgements**

620 We thank the European Commission's Horizon 2020 Programme as part of the MSCA-ITN  
621 project ArtMoMa under grant no. 860434, the FET-Open project MAGNIFY under grant no.  
622 801378, the LabEx CSC, the CNRS, and the University of Strasbourg. We wish to thank Prof.  
623 Christian Gauthier for fruitful discussions.

624

## 625 **Conflict of interests**

626 The authors declare no conflict of interests.

627

## 628 **References**

- 629 1 Schliwa, M. and Woehlke, G. (2003) Molecular motors. *Nature* 422, 759–765
- 630 2 Lindemann, C.B. and Lesich, K.A. (2010) Flagellar and ciliary beating: the proven and the  
631 possible. *J. Cell Sci.* 123, 519–528
- 632 3 Endow, S.A. *et al.* (2010) Kinesins at a glance. *J. Cell Sci.* 123, 3420–3424
- 633 4 Moulin, E. *et al.* (2020) From Molecular Machines to Stimuli-Responsive Materials. *Adv.*  
634 *Mater.* 32, 1906036
- 635 5 Giuseppone, N. and Walther, A. (2021) Out-of-Equilibrium (Supra)molecular Systems  
636 and Materials: An Introduction. In *Out-of-Equilibrium (Supra)molecular Systems and*  
637 *Materials* pp. 1–19, Wiley
- 638 6 Dattler, D. *et al.* (2020) Design of Collective Motions from Synthetic Molecular Switches,  
639 Rotors, and Motors. *Chem. Rev.* 120, 310–433
- 640 7 Beebe, D.J. *et al.* (2000) Functional hydrogel structures for autonomous flow control  
641 inside microfluidic channels. *Nature* 404, 588–590

- 642 8 Vázquez-González, M. and Willner, I. (2020) Stimuli-Responsive Biomolecule-Based  
643 Hydrogels and Their Applications. *Angew. Chem. Int. Ed.* 59, 15342–15377
- 644 9 Shi, J. *et al.* (2020) Responsive DNA-Based Supramolecular Hydrogels. *ACS Appl. Bio*  
645 *Mater.* 3, 2827–2837
- 646 10 Lu, C.-H. *et al.* (2015) Multitriggered Shape-Memory Acrylamide–DNA Hydrogels. *J. Am.*  
647 *Chem. Soc.* 137, 15723–15731
- 648 11 Yu, X. *et al.* (2016) Orthogonal Dual-Triggered Shape-Memory DNA-Based Hydrogels.  
649 *Chem. Eur. J.* 22, 14504–14507
- 650 12 Hu, Y. *et al.* (2016) Reversible Modulation of DNA-Based Hydrogel Shapes by Internal  
651 Stress Interactions. *J. Am. Chem. Soc.* 138, 16112–16119
- 652 13 Bruns, C.J. and Stoddart, J.F. (2016) *The Nature of the Mechanical Bond*, John Wiley &  
653 Sons, Inc.
- 654 14 Sluysmans, D. and Stoddart, J.F. (2019) The Burgeoning of Mechanically Interlocked  
655 Molecules in Chemistry. *Trends Chem.* 1, 185–197
- 656 15 Goujon, A. *et al.* (2017) Bistable [c2] Daisy Chain Rotaxanes as Reversible Muscle-like  
657 Actuators in Mechanically Active Gels. *J. Am. Chem. Soc.* 139, 14825–14828
- 658 16 Goujon, A. *et al.* (2019) [c2]Daisy Chain Rotaxanes as Molecular Muscles. *CCS Chem.* 1,  
659 83–96
- 660 17 Bi, Y. *et al.* (2020) Smart Bilayer Polyacrylamide/DNA Hybrid Hydrogel Film Actuators  
661 Exhibiting Programmable Responsive and Reversible Macroscopic Shape Deformations.  
662 *Small* 16, 1906998
- 663 18 Nakahata, M. *et al.* (2013) Redox-Generated Mechanical Motion of a Supramolecular  
664 Polymeric Actuator Based on Host-Guest Interactions. *Angew. Chem. Int. Ed.* 52, 5731–  
665 5735
- 666 19 Aramoto, H. *et al.* (2020) Redox-responsive supramolecular polymeric networks having  
667 double-threaded inclusion complexes. *Chem. Sci.* 11, 4322–4331
- 668 20 Greene, A.F. *et al.* (2017) Redox-Responsive Artificial Molecular Muscles: Reversible  
669 Radical-Based Self-Assembly for Actuating Hydrogels. *Chem. Mater.* 29, 9498–9508
- 670 21 Zhang, Y. *et al.* (2015) Fabrication of fluorescent holographic micropatterns based on  
671 the rare earth complexes using azobenzene-containing poly(aryl ether)s as  
672 macromolecular ligands. *J. Polym. Sci. Part A Polym. Chem.* 53, 936–943
- 673 22 Li, J. *et al.* (2020) Highly Bidirectional Bendable Actuator Engineered by LCST–UCST

- 674 Bilayer Hydrogel with Enhanced Interface. *ACS Appl. Mater. Interfaces* 12, 55290–  
675 55298
- 676 23 Lee, T.H. and Jho, J.Y. (2018) Temperature-Responsive Actuators Fabricated with  
677 PVA/PNIPAAm Interpenetrating Polymer Network Bilayers. *Macromol. Res.* 26, 659–  
678 664
- 679 24 Dong, L. and Zhao, Y. (2018) Photothermally driven liquid crystal polymer actuators.  
680 *Mater. Chem. Front.* 2, 1932–1943
- 681 25 Yang, Y. *et al.* (2016) Making and Remaking Dynamic 3D Structures by Shining Light on  
682 Flat Liquid Crystalline Vitrimer Films without a Mold. *J. Am. Chem. Soc.* 138, 2118–2121
- 683 26 Yang, H. *et al.* (2015) Near-infrared-responsive gold nanorod/liquid crystalline  
684 elastomer composites prepared by sequential thiol-click chemistry. *Chem. Commun.* 51,  
685 12126–12129
- 686 27 Wang, Y. *et al.* (2020) Repeatable and Reprogrammable Shape Morphing from  
687 Photoresponsive Gold Nanorod/Liquid Crystal Elastomers. *Adv. Mater.* 32, 2004270
- 688 28 Liu, L. *et al.* (2017) Near-Infrared Chromophore Functionalized Soft Actuator with  
689 Ultrafast Photoresponsive Speed and Superior Mechanical Property. *J. Am. Chem. Soc.*  
690 139, 11333–11336
- 691 29 Lahikainen, M. *et al.* (2018) Reconfigurable photoactuator through synergistic use of  
692 photochemical and photothermal effects. *Nat. Commun.* 9, 4148
- 693 30 Lahikainen, M. *et al.* (2020) Tunable Photomechanics in Diarylethene-Driven Liquid  
694 Crystal Network Actuators. *ACS Appl. Mater. Interfaces* 12, 47939–47947
- 695 31 Zhang, H. *et al.* (2020) Viewpoint: Pavlovian Materials—Functional Biomimetics  
696 Inspired by Classical Conditioning. *Adv. Mater.* 32, 1906619
- 697 32 Zeng, H. *et al.* (2020) Associative Learning by Classical Conditioning in Liquid Crystal  
698 Network Actuators. *Matter* 2, 194–206
- 699 33 Wang, C. *et al.* (2019) DNA-Based Hydrogels Loaded with Au Nanoparticles or Au  
700 Nanorods: Thermoresponsive Plasmonic Matrices for Shape-Memory, Self-Healing,  
701 Controlled Release, and Mechanical Applications. *ACS Nano* 13, 3424–3433
- 702 34 Yoshida, R. *et al.* (1996) Self-Oscillating Gel. *J. Am. Chem. Soc.* 118, 5134–5135
- 703 35 Masuda, T. *et al.* (2018) Chemomechanical Motion of a Self-Oscillating Gel in a Protic  
704 Ionic Liquid. *Angew. Chem. Int. Ed.* 57, 16693–16697
- 705 36 Yoshimura, K. *et al.* (2020) Autonomous oil flow generated by self-oscillating polymer

706 gels. *Sci. Rep.* 10, 12834

707 37 Kim, Y.S. *et al.* (2017) Recent developments in self-oscillating polymeric systems as  
708 smart materials: from polymers to bulk hydrogels. *Mater. Horizons* 4, 38–54

709 38 Yoshida, R. and Uesusuki, Y. (2005) Biomimetic Gel Exhibiting Self-Beating Motion in  
710 ATP Solution. *Biomacromolecules* 6, 2923–2926

711 39 Gelebart, A.H. *et al.* (2017) Mastering the Photothermal Effect in Liquid Crystal  
712 Networks: A General Approach for Self-Sustained Mechanical Oscillators. *Adv. Mater.*  
713 29, 1606712

714 40 Vantomme, G. *et al.* (2018) Self-sustained actuation from heat dissipation in liquid  
715 crystal polymer networks. *J. Polym. Sci. Part A Polym. Chem.* 56, 1331–1336

716 41 Vantomme, G. *et al.* (2021) Coupled liquid crystalline oscillators in Huygens' synchrony.  
717 *Nat. Mater.* DOI: 10.1038/s41563-021-00931-6

718 42 Wei, W. *et al.* (2018) Phototriggered Selective Actuation and Self-Oscillating in Dual-  
719 Phase Liquid Crystal Photonic Actuators. *Adv. Opt. Mater.* 6, 1800131

720 43 Kathan, M. and Hecht, S. (2021) Photoswitchable Components to Drive Molecular  
721 Systems Away from Global Thermodynamic Minimum by Light<sup>1</sup>. In *Out-of-Equilibrium*  
722 *(Supra)molecular Systems and Materials* pp. 275–304, Wiley

723 44 Boelke, J. and Hecht, S. (2019) Designing Molecular Photoswitches for Soft Materials  
724 Applications. *Adv. Opt. Mater.* 7, 1900404

725 45 Hou, J. *et al.* (2021) Photo-responsive Helical Motion by Light-Driven Molecular Motors  
726 in a Liquid-Crystal Network. *Angew. Chem. Int. Ed.* 60, 8251–8257

727 46 Bandara, H.M.D. and Burdette, S.C. (2012) Photoisomerization in different classes of  
728 azobenzene. *Chem. Soc. Rev.* 41, 1809–1825

729 47 Pilz da Cunha, M. *et al.* (2019) Unravelling the photothermal and photomechanical  
730 contributions to actuation of azobenzene-doped liquid crystal polymers in air and  
731 water. *J. Mater. Chem. C* 7, 13502–13509

732 48 Pilz da Cunha, M. *et al.* (2020) Bioinspired light-driven soft robots based on liquid crystal  
733 polymers. *Chem. Soc. Rev.* 49, 6568–6578

734 49 Koshima, H., ed. (2020) *Mechanically Responsive Materials for Soft Robotics*, Wiley.

735 50 Pang, X. *et al.* (2019) Photodeformable Azobenzene-Containing Liquid Crystal Polymers  
736 and Soft Actuators. *Adv. Mater.* 31, 1904224

737 51 Wu, Y. *et al.* (2020) Liquid-Crystalline Soft Actuators with Switchable Thermal

738 Reprogrammability. *Angew. Chem. Int. Ed.* 59, 4778–4784

739 52 Verpaalen, R.C.P. *et al.* (2020) Liquid Crystal Networks on Thermoplastics:  
740 Reprogrammable Photo-Responsive Actuators. *Angew. Chem. Int. Ed.* 59, 4532–4536

741 53 Wani, O.M. *et al.* (2019) An Artificial Nocturnal Flower via Humidity-Gated  
742 Photoactuation in Liquid Crystal Networks. *Adv. Mater.* 31, 1805985

743 54 Xiao, Y.-Y. *et al.* (2021) Desynchronized liquid crystalline network actuators with  
744 deformation reversal capability. *Nat. Commun.* 12, 624

745 55 Wani, O.M. *et al.* (2017) A light-driven artificial flytrap. *Nat. Commun.* 8, 15546

746 56 Wang, D. *et al.* (2018) Photoswitchable Azobenzene/Cyclodextrin Host-Guest  
747 Complexes: From UV- to Visible/Near-IR-Light-Responsive Systems. *ChemPhotoChem* 2,  
748 403–415

749 57 Iwaso, K. *et al.* (2016) Fast response dry-type artificial molecular muscles with [c2]daisy  
750 chains. *Nat. Chem.* 8, 625–632

751 58 Takashima, Y. *et al.* (2018) A Photoresponsive Polymeric Actuator Topologically Cross-  
752 Linked by Movable Units Based on a [2]Rotaxane. *Macromolecules* 51, 4688–4693

753 59 Klajn, R. (2014) Spiropyran-based dynamic materials. *Chem. Soc. Rev.* 43, 148–184

754 60 Satoh, T. *et al.* (2011) Fast-reversible light-driven hydrogels consisting of  
755 spirobenzopyran-functionalized poly(N-isopropylacrylamide). *Soft Matter* 7, 8030

756 61 Li, C. *et al.* (2020) Light-Driven Expansion of Spiropyran Hydrogels. *J. Am. Chem. Soc.*  
757 142, 8447–8453

758 62 Li, C. *et al.* (2020) Supramolecular–covalent hybrid polymers for light-activated  
759 mechanical actuation. *Nat. Mater.* 19, 900–909

760 63 Kobatake, S. *et al.* (2007) Rapid and reversible shape changes of molecular crystals on  
761 photoirradiation. *Nature* 446, 778–781

762 64 Irie, M. *et al.* (2014) Photochromism of Diarylethene Molecules and Crystals: Memories,  
763 Switches, and Actuators. *Chem. Rev.* 114, 12174–12277

764 65 Nakagawa, Y. *et al.* (2019) Photosalient Effect of Diarylethene Crystals of Thiazoyl and  
765 Thienyl Derivatives. *Chem. – A Eur. J.* 25, 7874–7880

766 66 Fujimoto, A. *et al.* (2020) Photoinduced swing of a diarylethene thin broad sword  
767 shaped crystal: a study on the detailed mechanism. *Chem. Sci.* 11, 12307–12315

768 67 Pezzato, C. *et al.* (2017) Mastering the non-equilibrium assembly and operation of  
769 molecular machines. *Chem. Soc. Rev.* 46, 5491–5507

770 68 Aprahamian, I. (2020) The Future of Molecular Machines. *ACS Cent. Sci.* 6, 347–358

771 69 Francis, W. *et al.* (2017) Spiropyran based hydrogels actuators—Walking in the light.  
772 *Sensors Actuators B Chem.* 250, 608–616

773 70 Li, C. *et al.* (2020) Supramolecular–covalent hybrid polymers for light-activated  
774 mechanical actuation. *Nat. Mater.* 19, 900–909

775 71 Yamada, M. *et al.* (2008) Photomobile Polymer Materials: Towards Light-Driven Plastic  
776 Motors. *Angew. Chem. Int. Ed.* 47, 4986–4988

777 72 Terao, F. *et al.* (2012) Light-Driven Molecular-Crystal Actuators: Rapid and Reversible  
778 Bending of Rodlike Mixed Crystals of Diarylethene Derivatives. *Angew. Chem. Int. Ed.*  
779 51, 901–904

780 73 Pilz da Cunha, M. *et al.* (2020) A Soft Transporter Robot Fueled by Light. *Adv. Sci.* 7,  
781 1902842

782 74 Palagi, S. *et al.* (2016) Structured light enables biomimetic swimming and versatile  
783 locomotion of photoresponsive soft microrobots. *Nat. Mater.* 15, 647–653

784 75 Kim, Y.S. *et al.* (2015) Thermoresponsive actuation enabled by permittivity switching in  
785 an electrostatically anisotropic hydrogel. *Nat. Mater.* 14, 1002–1007

786 76 Yuan, Y. *et al.* (2018) Self-assembled nematic colloidal motors powered by light. *Nat.*  
787 *Commun.* 9, 5040

788 77 Tong, F. *et al.* (2020) Light-Powered Autonomous Flagella-Like Motion of Molecular  
789 Crystal Microwires. *Angew. Chem. Int. Ed.* DOI: 10.1002/anie.202012417

790 78 Wilson, M.R. *et al.* (2016) An autonomous chemically fuelled small-molecule motor.  
791 *Nature* 534, 235–240

792 79 Kay, E.R. *et al.* (2007) Synthetic Molecular Motors and Mechanical Machines. *Angew.*  
793 *Chem. Int. Ed.* 46, 72–191

794 80 Feringa, B.L. (2001) In Control of Motion: From Molecular Switches to Molecular  
795 Motors. *Acc. Chem. Res.* 34, 504–513

796 81 Wilcken, R. *et al.* (2018) Complete Mechanism of Hemithioindigo Motor Rotation. *J. Am.*  
797 *Chem. Soc.* 140, 5311–5318

798 82 Eelkema, R. *et al.* (2006) Molecular machines: Nanomotor rotates microscale objects.  
799 *Nature* 440, 163

800 83 Chen, J. *et al.* (2018) Artificial muscle-like function from hierarchical supramolecular  
801 assembly of photoresponsive molecular motors. *Nat. Chem.* 10, 132–138

802 84 Leung, F.K.-C. *et al.* (2018) Supramolecular Packing and Macroscopic Alignment  
803 Controls Actuation Speed in Macroscopic Strings of Molecular Motor Amphiphiles. *J.*  
804 *Am. Chem. Soc.* 140, 17724–17733

805 85 Leung, F.K.-C. *et al.* (2019) Dual-Controlled Macroscopic Motions in a Supramolecular  
806 Hierarchical Assembly of Motor Amphiphiles. *Angew. Chem. Int. Ed.* 58, 10985–10989

807 86 Li, Q. *et al.* (2015) Macroscopic contraction of a gel induced by the integrated motion  
808 of light-driven molecular motors. *Nat. Nanotechnol.* 10, 161–165

809 87 Mariani, G. *et al.* (2020) Structural properties of contractile gels based on light-driven  
810 molecular motors: a small-angle neutron and X-ray study. *Soft Matter* 16, 4008–4023

811 88 Foy, J.T. *et al.* (2017) Dual-light control of nanomachines that integrate motor and  
812 modulator subunits. *Nat. Nanotechnol.* 12, 540–545

813 89 Orlova, T. *et al.* (2018) Revolving supramolecular chiral structures powered by light in  
814 nanomotor-doped liquid crystals. *Nat. Nanotechnol.* 13, 304–308

815